The ISME Journal (2016) 10, 2184–2197

www.nature.com/ismej

OPEN

ORIGINAL ARTICLE

Nitrification and its influence on biogeochemical cycles from the equatorial Pacific to the Arctic Ocean

Takuhei Shiozaki[1], Minoru Ijichi[1], Kazuo Isobe[2], Fuminori Hashihama[3], Ken-ichi Nakamura[4], Makoto Ehama[3], Ken-ichi Hayashizaki[5], Kazutaka Takahashi[4], Koji Hamasaki[1] and Ken Furuya[4]

[1]*Department of Marine Ecosystem Dynamics, Atmosphere and Ocean Research Institute, The University of Tokyo, Chiba, Japan;* [2]*Department of Applied Biological Chemistry, Graduate School of Agricultural and Life Sciences, The University of Tokyo, Tokyo, Japan;* [3]*Department of Ocean Sciences, Tokyo University of Marine Science and Technology, Tokyo, Japan;* [4]*Department of Aquatic Bioscience, Graduate School of Agricultural and Life Sciences, The University of Tokyo, Tokyo, Japan and* [5]*School of Marine Biosciences, Kitasato University, Kanagawa, Japan*

We examined nitrification in the euphotic zone, its impact on the nitrogen cycles, and the controlling factors along a 7500 km transect from the equatorial Pacific Ocean to the Arctic Ocean. Ammonia oxidation occurred in the euphotic zone at most of the stations. The gene and transcript abundances for ammonia oxidation indicated that the shallow clade archaea were the major ammonia oxidizers throughout the study regions. Ammonia oxidation accounted for up to 87.4% (average 55.6%) of the rate of nitrate assimilation in the subtropical oligotrophic region. However, in the shallow Bering and Chukchi sea shelves (bottom $\leqslant$67 m), the percentage was small (0–4.74%) because ammonia oxidation and the abundance of ammonia oxidizers were low, the light environment being one possible explanation for the low activity. With the exception of the shallow bottom stations, depth-integrated ammonia oxidation was positively correlated with depth-integrated primary production. Ammonia oxidation was low in the high-nutrient low-chlorophyll subarctic region and high in the Bering Sea Green Belt, and primary production in both was influenced by micronutrient supply. An ammonium kinetics experiment demonstrated that ammonia oxidation did not increase significantly with the addition of 31–1560 nM ammonium at most stations except in the Bering Sea Green Belt. Thus, the relationship between ammonia oxidation and primary production does not simply indicate that ammonia oxidation increased with ammonium supply through decomposition of organic matter produced by primary production but that ammonia oxidation might also be controlled by micronutrient availability as with primary production.
The ISME Journal (2016) **10,** 2184–2197; doi:10.1038/ismej.2016.18; published online 26 February 2016

Introduction

Nitrogen has a central role in biogeochemical cycles in the ocean because it generally limits marine biological production. New production, which is defined as production based on nitrogenous nutrients newly delivered from outside the productive layer (Dugdale and Goering, 1967), is balanced by the sinking particle flux in a steady-state system (Eppley and Peterson, 1979) and thus is used to evaluate the capacity of the biological pump.

Correspondence: Current address: T Shiozaki, Research and Development Center for Global Change, Japan Agency for Marine-Earth Science and Technology, 2-15, Natsushima, Yokosuka, Kanagawa 237-0061, Japan.
E-mail: takuhei.shiozaki@jamstec.go.jp
Received 21 August 2015; revised 3 January 2016; accepted 5 January 2016; published online 26 February 2016

The nitrate assimilation rate has been examined to determine new production because nitrate is considered the major allochthonous source of nitrogen, supplied to the euphotic zone from deep water (Falkowski *et al.*, 2003). Nitrification has been ignored because it is inhibited by sunlight (Olson, 1981; Guerrero and Jones, 1996). However, nitrification in the euphotic zone has been evaluated at the same time and has been found to be detectable (Ward *et al.*, 1989; Yool *et al.*, 2007; Clark *et al.*, 2008; Raimbault and Garcia, 2008; Beman *et al.*, 2012). These findings suggested that nitrate-based new production would be overestimated because of the occurrence of nitrification in the euphotic zone. Such surface nitrification is posing a challenge to our current understanding of the surface nitrogen cycle in the ocean. The environmental factors controlling nitrification are still poorly understood; hence, there

is large uncertainty in the estimation of nitrification and new production.

Nitrification has been considered to be a two-step process consisting of ammonia oxidation (ammonium to nitrite) followed by nitrite oxidation (nitrite to nitrate), and each step is carried out by different microbes. (Although very recent studies show that some bacteria belonging to genus *Nitrospira* perform both steps (Daims *et al.*, 2015; van Kessel *et al.*, 2015), the present study does not consider this process. The marker gene of the complete ammonia oxidizer is not found in the ocean in public databases (Daims *et al.*, 2015)). The first step of nitrification is the rate-limiting process, and it was formerly thought to be performed almost entirely by ammonia-oxidizing bacteria (AOB). Therefore, the limiting factors of nitrification in the ocean were thought to be tightly coupled with the physiological characteristics of AOB (Ward, 2002). However, ammonia-oxidizing archaea (AOA) belonging to the phylum Thaumarchaeota were discovered in the 2000s (Könneke *et al.*, 2005; Brochier-Armanet *et al.*, 2008), and subsequent studies found that AOA outnumber AOB in various regions, indicating that AOA could be a major ammonia-oxidizing organism (AOO) in the ocean (Wuchter *et al.*, 2006; Beman *et al.*, 2008, 2012; Church *et al.*, 2010). As an explanation for the abundant AOA, Martens-Habbena *et al.* (2009) suggested that the higher ammonium affinity of AOA compared with AOB could provide an advantage to AOA because ammonium concentration is typically low throughout most of the ocean. Few studies have investigated the transcript abundance of AOA in the ocean (Church *et al.*, 2010; Horak *et al.*, 2013; Urakawa *et al.*, 2014; Smith *et al.*, 2014), and little is known about the factors limiting their ammonia oxidation activities. A genome analysis (Walker *et al.*, 2010) demonstrated that AOA has different metabolic systems than AOB, suggesting that limiting factors for AOA could be different from those for AOB.

The regions studied in this research covered several biogeochemical provinces, from the equatorial Pacific to the Arctic Ocean; therefore, environmental conditions were expected to differ greatly among the provinces. We examined the influence of nitrification on the nitrogen cycle in the euphotic zone and the factors controlling ammonia oxidation via large-scale observations. We investigated ammonia oxidation and the nitrate assimilation rate simultaneously. Furthermore, we examined the kinetics of ammonium utilization for ammonia oxidation in each oceanic region and determined the ammonium concentration at the nanomolar level using supersensitive colorimetric methods onboard a vessel (Hashihama *et al.*, 2015; Kodama *et al.*, 2015). We also determined the ammonia monooxygenase subunit A (*amoA*) gene and the transcript abundances of AOB and shallow and deep clades of AOA, for which the affinity to ammonium and the distribution are considered to be different.

Materials and methods

Sampling was performed onboard the R/V *Hakuho-Maru* (KH-14-3) from 23 June to 11 August 2014 in the North Pacific Ocean and the Arctic Ocean (Figure 1). A depth profile of light intensity was determined just prior to each water sampling using a Hyper Profiler (Satlantic LP, Halifax, NS, Canada) at all stations except Sts.1, 2 and 3; at these stations, observations were carried out only at night due to time constraints and thus the light profile was assumed to be the same as that estimated in the same region and during the same season during the KH-12-3 cruise. Temperature, salinity and dissolved oxygen profiles were measured using a SBE 911 plus CTD system (Sea-Bird Electronics, Inc., Washington, DC, USA). Water samples were collected by an acid-cleaned bucket from the surface and by acid-cleaned Teflon-coated 12 l Niskin-X bottles from other depths. Samples for nutrients and chlorophyll *a* were collected from depths corresponding to 100%, 25%, 10%, 1%, 0.3% and 0.1% of the surface light intensity and from the depth of 200 m. In addition, samples for chlorophyll *a* were taken from depths of 5, 10, 20, 30, 50, 75, 100, 125, 150, 250 and 300 m. Samples for experiments of primary production and nitrate assimilation were collected from the five light depths

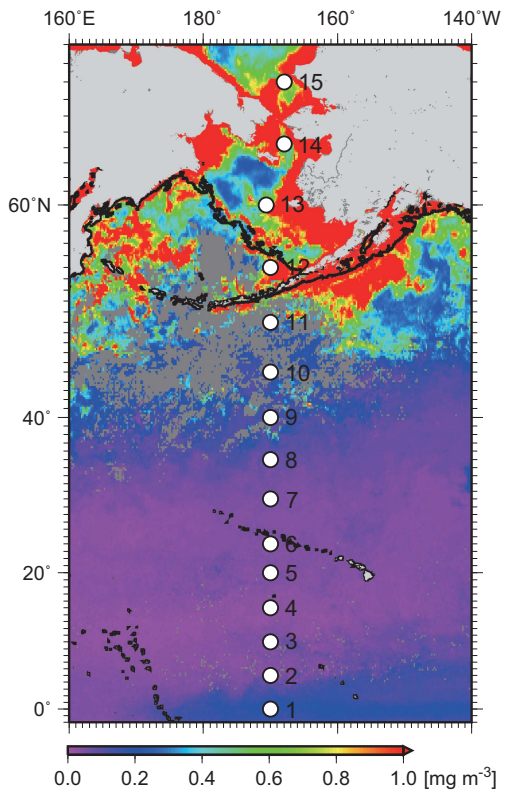

Figure 1 Sampling stations in the North Pacific Ocean and Arctic Ocean during the KH-14-3 cruise. The background contour represents satellite-derived chlorophyll *a* during the study period. Black lines denote 200-m isobaths. Gray areas in the ocean indicate no data.

corresponding to 100%, 25%, 10%, 1% and 0.1% of the surface light intensity. Samples for the experiments of ammonia oxidation and DNA analyses were collected from the depths corresponding to 100%, 10%, 1%, 0.3% and 0.1% of the surface light intensity and from the depth of 200 m. Samples for RNA analyses were taken only from the 0.1% light depth. As primary production generally increases near the surface, samples for the primary production and nitrate assimilation experiment were mainly collected from shallow depths. In contrast, maximum ammonia oxidation occurs around the bottom of the euphotic zone (Beman *et al*., 2008, 2012), and thus, samples for ammonia oxidation experiment were mainly collected from deeper water.

Nutrients and chlorophyll a

Samples for nutrients analysis were collected in single acid-cleaned 30-ml polypropylene tubes and in duplicate 10-ml acrylic tubes. The samples in the 10-ml acrylic tubes were kept frozen until analysis onshore. At Sts.1–6, which correspond with the leg 1 cruise of KH-14-3, the concentrations of nitrate, nitrite, ammonium and phosphate were determined immediately onboard at the nanomolar level using supersensitive colorimetric systems (Hashihama *et al*., 2009, 2015). The detection limits were 3, 2, 4 and 3 nM, respectively. At Sts. 7–15, which correspond with the leg 2 cruise of KH-14-3, only ammonium concentration was determined onboard using a highly sensitive and large concentration range colorimetric analysis (Kodama *et al*., 2015). The detection limit of this analysis was 6 nM. The concentrations of nitrate, nitrite and phosphate at Sts. 7–15 were determined at the nanomolar level on land using the supersensitive colorimetric systems (Hashihama *et al*., 2009). When the concentrations of nitrate, nitrite and phosphate were higher than 1 μM, they were determined using an AACSII auto-analyzer.

Samples for chlorophyll *a* were filtered using 25 mm Whatman GF/F filters, and the chlorophyll *a* concentrations were determined onboard using a Turner Design 10-AU fluorometer after extraction with *N*, *N*-dimethylformamide.

Ammonia oxidation

Samples for the ammonia oxidation experiment were collected in duplicate in acid-cleaned 0.3 l polycarbonate (PC) bottles. ^{15}N-labeled ammonium sulfate (99 atom% ^{15}N; SI Science) was spiked to give a final tracer concentration of 31 nM. In addition, to examine the kinetics of ammonia oxidation, the ^{15}N-labeled ammonium sulfate was spiked to the samples collected from the 0.1% light depth to adjust the final tracer concentrations to 31, 62, 234 and 1560 nM. The atom% ^{15}N and ammonia oxidation rate in each incubation bottle are listed in Supplementary Table S1. The samples from 200 m were covered with black screen and those from the other depths were covered with neutral-density screens to adjust the light levels (10%, 1%, 0.3% and 0.1%). Those bottles were incubated in a thermostatic incubator (CN-25B, MEE) whose temperature was adjusted to the sea temperature of the 0.3% light depth under 150 μmol photons m^{-2} s^{-1} light intensity. The light and dark cycle was adjusted to the cycle at each station. Samples collected from the surface water were incubated without a screen in the on-deck incubator. After 24 h incubation, the filtrate passing through a 0.2 μm pore size cellulose acetate in-line filter (DISMIC, ADVANTEC MFS, Inc., Tokyo, Japan) was collected in 50-ml polypropylene bottles and in 10-ml acrylic tubes and was kept frozen until analysis. Analysis of the δ^{15}N of nitrate+nitrite in the filtrate was performed using the denitrifier method (Sigman *et al*., 2001; Isobe *et al*., 2011). In brief, 10-ml filtrate was dispensed into a 50-ml vial, purged for 10 min with ultrapure He, and inoculated with 2 ml concentrated medium of nitrate-starved *Pseudomonas chlororaphis* subsp. *aureofaciens* ATCC13985, which was also purged for 2 h with ultrapure He. The reaction was terminated by adding 1 ml 8 M NaOH after 24 h incubation to allow complete conversion of nitrate+nitrite into N_2O. The N_2O that was produced was injected into a GasBench II equipped with a cold trap system for concentration and purification and then introduced into a DELTA^{plus} XP isotope ratio mass spectrometer. The s.d.s of the δ^{15}N values measured for the 1000 and 100 nM nitrate standards were 0.49‰ and 2.12‰, respectively. The concentration of nitrate+nitrite in the filtrate was determined by colorimetry using an AACSII auto-analyzer (Bran+Luebbe, Norderstedt, Germany). Ammonia oxidation rates were calculated using the equation given by Beman *et al*. (2012).

We defined detectable activity as when the difference between δ^{15}N-nitrate in the incubated and initial samples was more than threefold the s.d. of the nitrate standard. Hence, when the nitrate concentration was >1000 nM, we considered that ammonia oxidation was detectable when the difference was >1.47‰. When the nitrate concentration was 100–1000 nM, the difference was set >6.36‰. Furthermore, we regarded ammonia oxidation to be below the detection limit when the nitrate concentration was <100 nM. At St. 15, the ambient ammonium concentration at the 0.1% light depth was too high (5540 nM) to detect ammonia oxidation at the final tracer concentrations of 31 and 62 nM. Meanwhile, the ammonia oxidation rates for 234 and 1560 nM were 5.01 and 5.16 nmol$N$ l^{-1} d^{-1}, respectively, and the ammonia oxidation at that depth was taken as the mean of these values.

Primary production and nitrate assimilation rates

Samples for the primary production experiment were collected in duplicate in acid-cleaned 4.5 l PC bottles. Primary production was measured with nitrogen fixation using a dual (^{15}N and ^{13}C) isotopic

technique (nitrogen fixation data are not shown here). ^{13}C-labeled sodium bicarbonate (99 atom% ^{13}C; Cambridge Isotope Laboratories, Inc., Andover, MA, USA) was added to each bottle at a final tracer concentration of 200 μmol l^{-1}. After $^{15}N_2$-dissolved water was added to the bottle, it was sealed with a thermoplastic elastomer cap. Samples for the nitrate assimilation experiment were collected in acid-cleaned 2 l PC bottles. At Sts. 2–8, 14 and 15, nitrate assimilation was estimated by the Michaelis–Menten kinetics approach to correct the overestimation caused by the excessive use of the ^{15}N tracer (Kanda *et al.*, 2003; Shiozaki *et al.*, 2009); ^{15}N-labeled nitrate (99 atom% ^{15}N; SI Science) was added to each bottle to adjust the final tracer concentrations to 10, 22, 109 and 2170 nM. The enrichment of ^{15}N-labeled nitrate at the other stations was: 109 nM at St.1, 217 nM at St. 9–11, 1090 nM at St.12 and 435 nM at St. 13. The atom% ^{15}N and nitrate assimilation rates in each incubation bottle are listed in Supplementary Table S2. The bottles for the primary production and the nitrate assimilation experiments were covered with neutral-density screen to adjust the light levels (100%, 25%, 10%, 1% and 0.1%) and then incubated in an on-deck incubator cooled by flowing surface seawater. Where the bottles for primary production were incubated for 24 h, those for nitrate assimilation were incubated for 2–3 h during daytime. At Sts. 3, 8 and 11, samples for nitrate assimilation were collected from the water column during both daytime and nighttime and were immediately incubated with ^{15}N-labeled nitrate. At the other stations, samples for night-time incubation were collected from the surface, incubated without ^{15}N tracer in the on-deck incubator until midnight, and then ^{15}N-labeled nitrate was added. The night-time incubations were also performed for 2–3 h. Although ammonia oxidation is less susceptible to temperature (Horak *et al.*, 2013; Baer *et al.*, 2014), primary production and nitrate assimilation are significantly influenced by temperature (Harrison *et al.*, 1996; Behrenfeld and Falkowski, 1997). Although these properties are not linearly related to temperature and the deviation from the actual value is difficult to estimate, there is the possibility of bias in these rates measured using the on-deck incubations. Incubation was terminated by gentle vacuum filtration of the seawater samples through precombusted GF/F filters. Analyses and calculations were performed as described previously (Shiozaki *et al.*, 2009, 2011). The s.d. of the δ^{15}N values of a working standard (L-alanine) was <0.3‰.

DNA and RNA sampling and extraction

Samples (2 l) for RNA and DNA analyses were filtered onto Sterivex-GP pressure filter units with a 0.22 μm pore size (Millipore, Billerica, MA, USA). RNA samples were filtered within 30 min of the water sampling and then added to RNA*later* Stabilization Solution (Life Technologies, Carlsbad, CA, USA). The Sterivex filter units were frozen at − 80 °C until onshore analyses. Total DNA was extracted using a ChargeSwitch Forensic DNA Purification Kit (Invitrogen, Carlsbad, CA, USA). For RNA extraction, a *mir*Vana miRNA Isolation Kit (Life Technologies) was used after the RNA*later* solution in the Sterivex filter units was removed. Then the extracted RNA was treated with the Turbo DNA Free Kit (Ambion, Austin, MD, USA) to remove contaminating DNA. The concentration of the purified RNA was measured using Nano Drop 2000 (Thermo Scientific, Waltham, MA, USA). Complementary DNA synthesis was performed using Transcriptor First Strand cDNA Synthesis Kit (Roche Applied Science, Mannheim, Germany) with random hexamer as the primer. Sample treatment using the kits followed the manufacturer's instructions.

Quantitative polymerase chain reaction analyses

AOA have been classified into three major groups in the ocean based on their *amoA* gene sequences: the *Nitrosopumilus maritimus*-like cluster, water column cluster A and water column cluster B (Francis *et al.*, 2005; Beman *et al.*, 2008). As the water column cluster A is dominant in surface water, this cluster is also called the shallow clade (Hallam *et al.*, 2006). Based on the *AmoA* sequences, the *Nitrosopumilus maritimus*-like cluster is also included in the shallow clade (Hallam *et al.*, 2006; Beman *et al.*, 2008). In contrast, water column cluster B is found only in deep water, and hence, is called the deep clade (Hallam *et al.*, 2006). The primer set Arch-amoAFA & Arch-amoAR that we used in this study covers both water column cluster A and the *Nitrosopumilus maritimus*-like cluster, namely the shallow clade (Beman *et al.*, 2008). Further, the primer set Arch-amoAFB & Arch-amoAR covers water column cluster B, namely the deep clade (Beman *et al.*, 2008). To avoid confusion of terminology, we denoted the quantified AOA using Arch-amoAFA & Arch-amoAR and Arch-amoAFB & Arch-amoAR as the shallow and deep clades, respectively. The primer sets that we used did not target the water column cluster C and soil assemblages, which are minor groups in the marine water column (Francis *et al.*, 2005). Therefore, we might miss these contributions if these groups dominated in the samples.

AOB have been classified into two groups: Betaproteobacteria and Gammaproteobacteria. We used the primer sets amoA-1F & amoA-r-NEW for Betaproteobacteria (hereafter βAOB) (Hornek *et al.*, 2006) and amoA-3F & amoA-4R for Gammaproteobacteria (Purkhold *et al.*, 2000). When we applied quantitative PCR assay to gammaproteobacterial *amoA* gene, non-specific bands were detected from most of the PCR products. Therefore, we only quantified βAOB.

The quantitative PCR assays were performed on a LightCycler 480 Real-Time PCR System (Roche

Applied Science). The reaction mixtures (20 µl) contained 10 µl SYBR Premix Ex Taq (TaKaRa, Shiga, Japan), 0.2 µM each primer and 1 µl DNA. The assays were run in triplicate under the following cycling conditions: 95 °C for 30 s, followed by 45 cycles of 95 °C for 15 s; 56 °C (shallow clade AOA), 55 °C (deep clade AOA) or 55 °C (βAOB) for 30 s; and 72 °C for 30 s; with a detection step at the end of each cycle. The primer (and relevant references), quantitative PCR standards, standard curve correlation coefficients, PCR efficiencies and detection limits are listed in Supplementary Table S3.

Results

Biogeochemical provinces and environmental conditions

We classified oceanic regions according to temperature, salinity, surface chlorophyll *a* concentration and geographical location (Longhurst, 2007) (Figures 2a–c and Supplementary Figure S1). High surface chlorophyll *a* at St. 1 indicated that this station was located in the Pacific Equatorial Divergence Province (PEQD). Surface salinity at St. 2 was lower than at surrounding stations, suggesting that this station was in the North Pacific Equatorial Countercurrent Province (PNEC). The North Pacific Tropical Gyre Province (NPTG) extended from St. 3 to St. 8. Surface nitrate was depleted from St. 2 to St. 8 (Figure 2d and Table 1). Temperature and salinity at the surface changed markedly from St. 8 to St. 10, and the temperature and salinity at St. 10 were typical of values in the Pacific Subarctic Gyres Province (PSAG) in summer (Longhurst, 2007). Therefore, St. 9 was located in the North Pacific Subtropical and Polar Front Provinces (NPST/NPPF). The surface nitrate concentration at St. 9 (305 nM) was somewhat low compared with those in the PSAG (>1000 nM; Harrison *et al*., 2004). Although the temperature-salinity diagram indicated that St. 11 was close to St. 12 (Supplementary Figure S1), St. 11 was classified as PSAG from its geographical location. The surface nitrate concentration at Sts. 10 and 11 was very high (9950 and 7570 nM, respectively). To the north of St. 12, stations were divided into the North Pacific Epicontinental Sea Province (BERS; Sts. 12–14) and the Boreal Polar Province (BPLR; St. 15) according to the geographical location. The surface nitrate concentrations at Sts. 13 and 14 were almost depleted (<3 and 5 nM, respectively), and those at Sts. 12 and 15 were 435 and 211 nM, respectively.

Nitrite had a clear subsurface maximum throughout the study regions, except at Sts. 1 and 14 (Figure 2e). The primary nitrite maximum was

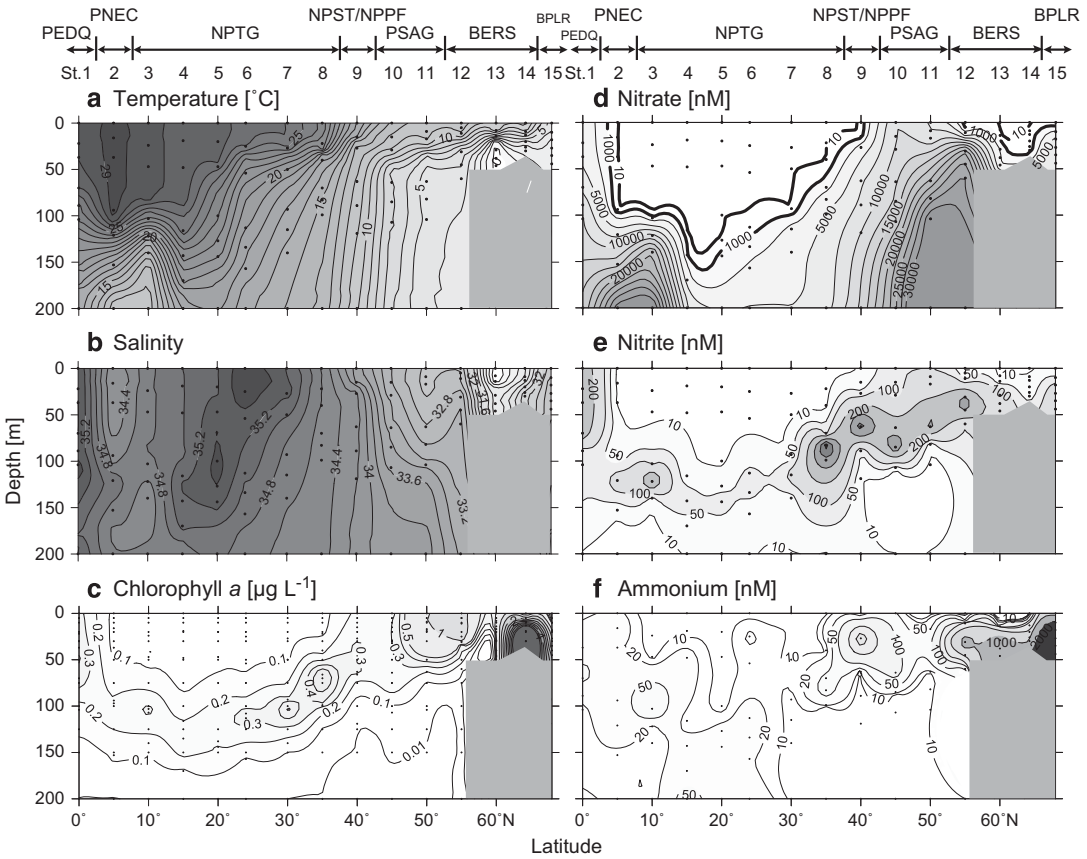

Figure 2 Vertical profiles of (**a**) temperature (°C), (**b**) salinity, (**c**) chlorophyll *a* (µg l^{-1}), (**d**) nitrate (nM), (**e**) nitrite (nM) and (**f**) ammonium (nM) along the transect from the equatorial Pacific to the Arctic Ocean.

Table 1 Environmental variables at the surface (SST, chlorophyll *a*, and nitrate), depth-integrated biological activities (primary production, nitrate [NO_3^-] assimilation and ammonia [NH_3] oxidation) and contribution of nitrification to nitrate assimilation at each station

Station	*Region*	*Date (local time)*	*SST (°C)*	*Chl a ($\mu g\,l^{-1}$)*	*Nitrate (nM)*	*Primary production ($mmol\,C\,m^{-2}\,d^{-1}$)*	*NO_3^- assimilation ($mmolN\,m^{-2}\,d^{-1}$)*	*NH_3 oxidation ($mmolN\,m^{-2}\,d^{-1}$)*	*Contribution of nitrification (%)*
1	PEQD	Jul 3	28.1	0.33	4100	70.9 (68.2)	10.9 (9.48)	0.79 (0.21)	7.22 (2.19)
2	PNEC	Jul 4	28.6	0.07	<3	16.2 (14.1)	1.17 (0.08)	0.49 (n.d.)	41.5 (0)
3	NPTG	Jul 6	28.2	0.09	<3	28.2 (26.3)	2.65 (0.25)	0.22 (n.d.)	8.13 (0)
4	NPTG	Jul 7	27.0	0.06	<3	21.9 (18.8)	0.38 (0.07)	0.33 (n.d.)	87.4 (0)
5	NPTG	Jul 9	27.3	0.07	<3	19.8 (17.2)	0.20 (0.07)	0.11 (n.d.)	56.8 (0)
6	NPTG	Jul 10	26.6	0.05	<3	34.1 (30.6)	0.69 (0.35)	0.53 (0.10)	76.2 (28.4)
7	NPTG	Jul 20	26.6	0.06	<3	15.6 (14.1)	0.47 (0.08)	0.37 (n.d.)	78.6 (0)
8	NPTG	Jul 21	24.2	0.07	<3	26.8 (22.5)	0.80 (0.23)	0.32 (0.001)	40.7 (0.55)
9	NPST/NPPF	Jul 23	17.6	0.22	305	40.2 (36.7)	2.90 (1.81)	1.71 (0.40)	59.0 (21.9)
10	PSAG	Jul 24	12.9	0.25	9950	27.8 (25.8)	2.90 (2.18)	0.35 (0.03)	12.1 (1.52)
11	PSAG	Jul 25	12.3	0.96	7570	52.7 (51.6)	9.10 (5.74)	1.08 (0.33)	11.9 (5.80)
12	PSAG	Jul 26	11.6	1.28	435	49.2 (47.5)	7.15 (5.22)	1.90 (0.40)	26.6 (7.65)
13	BERS	Jul 28	10.0	0.52	<3	20.4 (18.9)	1.33 (1.00)	0.06 (0.02)	4.74 (1.86)
14	BERS	Jul 29	10.3	0.47	5	87.8 (76.0)	26.1 (23.8)	n.d. (n.d.)	0 (0)
15	BPLR	Jul 30	5.6	0.12	211	11.0 (10.1)	1.70 (1.54)	0.02 (n.d.)	1.18 (0)

Abbreviations: BERS, the North Pacific Epicontinental Sea Province; BLPR, the Borreal Polar Province; n.d., not detected; NPTG, North Pacific Tropical Gyre Province; NPST/NPPF, North Pacific Subtropical and Polar Front Provinces; PEQD, Pacific Equatorial Divergence Province; PNEC, the North Pacific Equatorial Countercurrent Province; PSAG, the Pacific Subarctic Gyres Province.
Number in parentheses indicates depth-integrated value to the 1% light depth.

emerged in deep water in the subtropical region but tended to shoal to the north (Supplementary Figure S2a). The concentration at the nitrite maximum varied between 65 and 554 nM.

The subsurface ammonium maximum was not very significant from the PEQD to the PSAG (Figure 2f). In contrast, in the BERS and BPLR, the ammonium concentration clearly increased at the subsurface or near the bottom, and the maximum concentrations at Sts. 12, 13, 14 and 15 were 1380 nM (31 m), 1650 nM (38 m), 950 nM (26 m) and 5740 nM (44 m), respectively.

The subsurface chlorophyll *a* maximum (SCM) was developed in the study region, except in the PSAG and at St. 12 in the BERS. Although the depth of the SCM deepened in the NPTG and became shallow to the north, as for the nitrite maximum, the SCM tended to be shallower than the nitrite maximum (Supplementary Fig. S2a). At Sts. 14 and 15 in the BERS and BPLR, the SCM occurred in the deepest water, near the bottom. The surface chlorophyll *a* concentrations at Sts. 10 and 11 (0.25 and 0.96 $\mu g\,l^{-1}$, respectively) were lower than that at St. 12 (1.28 $\mu g\,l^{-1}$), whereas the surface nitrate concentrations at Sts. 10 and 11 (9950 and 7570 nM, respectively) were an order of magnitude higher than that at St. 12 (435 nM) (Table 1), suggesting that Sts. 10 and 11 were located in a high-nutrient low-chlorophyll region.

Ammonia oxidation, primary production and nitrate assimilation

Ammonia oxidation occurred at all stations except St. 14, and the peak in the water column was below the 1% light depth (Figure 3a). Ammonia oxidation at the 100% light depth was detected at only St. 1, and that at the 10% light depth was found only at Sts. 1, 9, 12 and 15. The peak of ammonia oxidation was below the SCM, except at St. 15 (Supplementary Figure S2a), and it varied from 2.87 to 67.1 $nmolN\,l^{-1}\,d^{-1}$. The depth-integrated rate to the 0.1% light depth varied from 0.02 to 1.90 $mmolN\,m^{-2}\,d^{-1}$ (Table 1). The depth-integrated rates in the PNEC and NPTG (0.11–0.53 $mmolN\,m^{-2}\,d^{-1}$) were lower than those in the surrounding regions (0.79 $mmolN\,m^{-2}\,d^{-1}$ in the PEQD and 1.71 $mmolN\,m^{-2}\,d^{-1}$ in the NPST/NPPF). North of the NPST/NPPF, the depth-integrated value at St.10 (0.35 $mmolN\,m^{-2}\,d^{-1}$) was lower than the value at the adjacent stations (1.08 $mmolN\,m^{-2}\,d^{-1}$ at St. 11). The highest ammonia oxidation value (67.1 $nmolN\,l^{-1}\,d^{-1}$) occurred at St. 12 in the BERS. Ammonia oxidation was low at Sts. 13, 14 and 15 (<5.08 $nmolN\,l^{-1}\,d^{-1}$). The kinetics experiment at the 0.1% light depth demonstrated that substantial elevation of ammonia oxidation with addition of ^{15}N-labeled ammonium was observed only at St. 12 among Sts. 1–12 (Figure 4a). At St. 8, ammonia oxidation was slightly elevated with the addition of the ^{15}N tracer.

The maximum primary production generally occurred at the surface, except at Sts. 3, 14 and 15, and ranged between 255 and 8270 $nmolC\,l^{-1}\,d^{-1}$. Primary production was detected but was low at the 0.1% light depth (3–46 $nmolC\,l^{-1}\,d^{-1}$), except at St. 14 (505 $nmolC\,l^{-1}\,d^{-1}$) (Figure 3b). The euphotic zone is conventionally defined from the surface down to the 1% light depth, below which no appreciable photosynthesis can occur (Ryther,

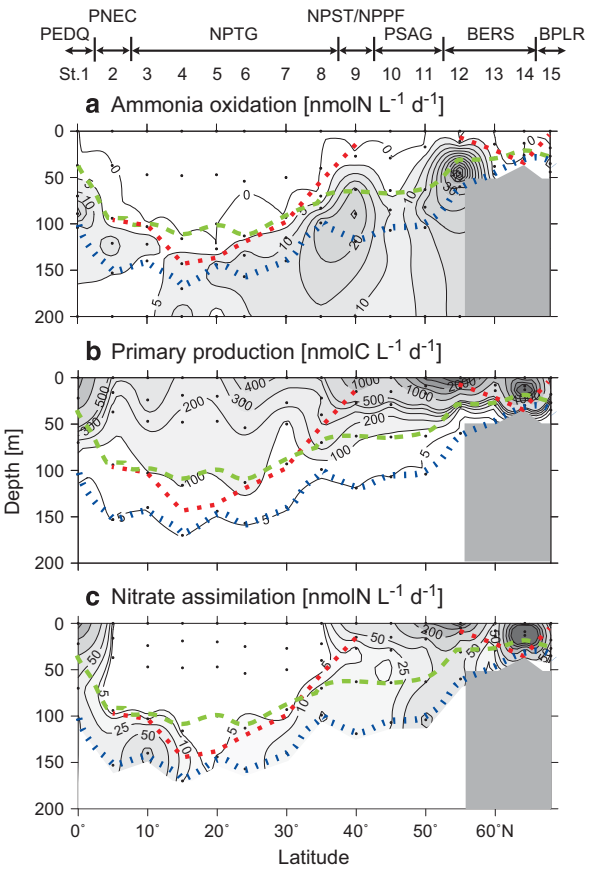

Figure 3 Vertical profiles of (**a**) ammonia oxidation (nmolN l^{-1} d^{-1}), (**b**) primary production (nmolC l^{-1} d^{-1}) and (**c**) nitrate assimilation (nmolN l^{-1} d^{-1}) along the transect from the equatorial Pacific to the Arctic Ocean. Dashed lines indicate the 1% light depth (green), the 0.1% light depth (blue) and the nitracline depth (red), respectively.

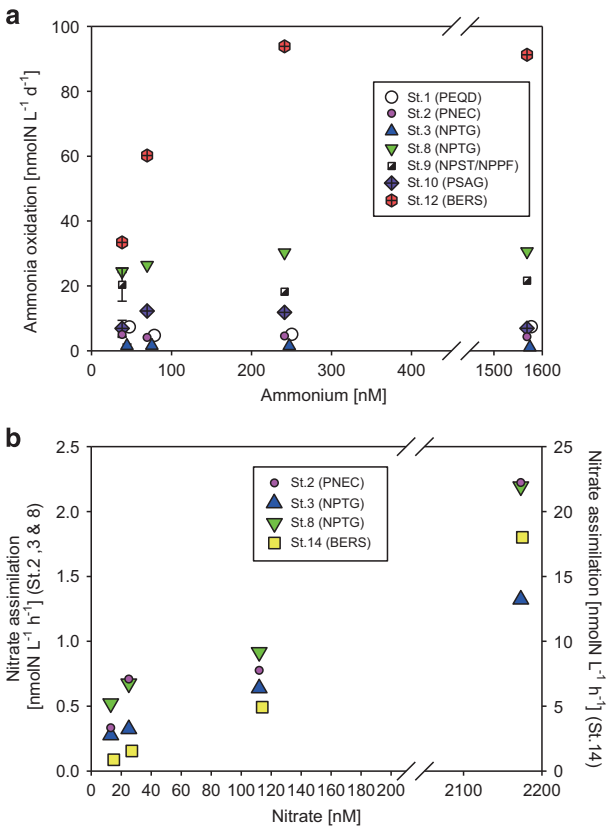

Figure 4 Selected results of the kinetics experiments for (**a**) ammonia oxidation (Sts. 1, 2, 3, 8, 9, 10 and 12) and (**b**) nitrate assimilation (Sts. 2, 3, 8 and 14). Each station was a representative in each region. The horizontal axes indicate total substrate concentration (^{15}N tracer addition+ambient substrate concentration).

1956). In this study, according to the results of primary production, the euphotic zone was defined down to the 0.1% light depth. Therefore, unless otherwise noted, productivity per area is integrated from the surface to the 0.1% light depth.

Nitrate assimilation was always stimulated by the addition of nitrate, ranging from 10 to 2170 nM in the depths where ambient nitrate concentration was almost depleted (⩽31 nM; Figure 4b). Nitrate assimilation in the study regions showed a maximum at the surface in the PEQD, NPST/NPPF, PSAG, and at Sts. 12 and 13 in the BERS. (Figure 3c). In the PNEC and NPTG, the maximum nitrate assimilation occurred at the 0.1% light depth, which was always placed below the nitracline. The maximum values and depth-integrated values varied as 5.30–2280 nmolN l^{-1} d^{-1} and 0.20–26.1 mmolN m^{-2} d^{-1} (Table 1), respectively. At St. 14, although ambient nitrate concentration was low (<500 nM) throughout the entire water column, the maximum nitrate assimilation (1980 nmolN l^{-1} d^{-1}) was the highest value in the study regions, suggesting that supplied nitrate was rapidly consumed by microbes at this site. The depth-integrated nitrate assimilation was positively related with nitrate concentration, except for the data collected at St. 14 ($r=0.72$, $P<0.05$) (Figure 5a), and was positively correlated with primary production throughout the whole region ($r=0.91$, $P<0.05$) (Figure 5b).

The ratio of ammonia oxidation to nitrate assimilation was significantly higher in the PNEC and NPTG (average 55.6%) than in the other regions (Table 1). The highest ratio (87.4%) was observed at St. 4.

amoA abundance and expression

Shallow clade AOA were detected at all stations except St. 14 and had a subsurface maximum within the depth of 200 m (Figure 6a and Supplementary Figure S2b). At St. 7, the maximum occurred at 200 m. Shallow clade AOA were not observed in the surface water at Sts. 5–14. The abundance of shallow clade AOA varied from 590 to 33×10^6 copies l^{-1} at all stations, and at Sts. 13–15, the values (from below detection limit to 0.0043×10^6 copies l^{-1}) tended to be lower than those in the other regions. The maximum in the PNEC and NPTG (average 7.95 (±4.57) $\times10^6$ copies l^{-1}) was lower than those in the neighboring regions: the PEQD (12.5×10^6 copies l^{-1})

and the NPST/NPPF (16.5×10^6 copies l^{-1}). The depth of the subsurface maximum did not correspond with that of ammonia oxidation at most stations (Supplementary Figure S2b).

Deep clade AOA were detected in the study region, except at Sts. 13–15, and occurred only below the 1% light depth (Figure 6b). The maximum abundance of deep clade AOA was always placed at 200 m at the stations (Supplementary Figure S2b), ranged between 0.36×10^6 and 12.8×10^6 copies l^{-1}, and there was no apparent difference among the study regions. The abundance of deep clade AOA exceeded that of shallow clade AOA only at the 200 m depth of Sts. 1–3.

βAOB were detected at the stations, except for Sts. 2–5 and 14 (Figure 6c). They were observed at the surface only at Sts. 8 and 10. The vertical distribution of βAOB showed a subsurface maximum at the each station, and at Sts. 7 and 8, the maximum occurred at 200 m (Supplementary Figure S2b). The maximum βAOB abundance ranged between 0.0024×10^6 and 1.31×10^6 copies l^{-1}. The maximum depth did not match the depth of maximum ammonia oxidation at most stations. North of the NPST/NPPF, the abundance of βAOB was higher than that of deep clade AOA at the depth of the βAOB maximum. The abundance of βAOB was generally one order of magnitude lower than that of shallow clade AOA, except at St. 13 where their abundances were comparable and the ratio of shallow clade AOA to βAOB at the depth of the βAOB maximum was 1.43. The ratio of AOA to βAOB tended to be low in ammonium-rich water (Figure 6d).

Except at St. 14, *amoA* expression was detected at all stations, and that of shallow clade AOA always exceeded that of deep clade AOA and βAOB (Figure 7a). The *amoA* expression of shallow clade AOA varied from 0.004×10^6 to 0.33×10^6 transcripts l^{-1} at Sts. 1–7, and it increased from St. 8 (1.05×10^6 transcripts l^{-1}) to St. 12 (3.94×10^6 transcripts l^{-1}), except at St. 10 where it decreased to 0.22×10^6 transcripts l^{-1}. At Sts. 13 and 15, the *amoA* expression of shallow clade AOA was low at 0.099×10^6 and 0.013×10^6 transcripts l^{-1}, respectively. Although the *amoA* gene of deep clade AOA was detected at Sts. 1–11, expression was found only at Sts. 1, 6, 7, 9 and 11, with a value of $0.018–0.13 \times 10^6$ transcripts l^{-1}. βAOB *amoA* expression was observed only at Sts. 9, 11, 12 and 13, where it varied from 0.0065×10^6 to 0.087×10^6 transcripts l^{-1}. At St. 13, the *amoA* expression of βAOB (0.087×10^6 transcripts l^{-1}) was comparable to that of shallow clade AOA (0.099×10^6 transcripts l^{-1}).

At the 0.1% light depth, the *amoA* gene abundance of shallow clade AOA was positively but weakly related with ammonia oxidation ($\rho = 0.63$, $P < 0.05$, Spearman rank correlation) (Figure 7b). In addition, the abundance of βAOB was positively related with ammonia oxidation ($\rho = 0.56$, $P < 0.05$) (Figure 7b). There was no relationship between the abundance of deep clade AOA and ammonia oxidation at that depth ($\rho = 0.11$, $P > 0.05$) (Figure 7b). The *amoA* expression of shallow clade AOA was positively and strongly related with ammonia oxidation ($\rho = 0.79$, $P < 0.001$; Figure 7c). The *amoA* expressions of deep clade AOA and βAOB were not correlated with ammonia oxidation ($\rho = 0.19$ and $\rho = 0.29$, respectively, $P > 0.05$) (Figure 7c).

Discussion

Distribution of ammonia oxidation and AOO and influence of nitrification on nitrate assimilation

Although studies on ammonia oxidation in the open ocean remain limited, our measurements obtained from various environments are in accordance with those of previous studies. In the PEQD, Raimbault *et al.* (1999) reported that the maximum ammonia oxidation ranged between ca. 20 and 40 nmolN l^{-1} d^{-1}, and our estimate (24.5 nmolN l^{-1} d^{-1}) was within this range. Ammonia oxidation in the subtropical oligotrophic region of the Atlantic Ocean was found to vary from 1 to 10 nmolN l^{-1} d^{-1} (Clark *et al.*, 2008; Newell *et al.* 2013), which is similar to the values we found (1.53–24.4 nmolN l^{-1} d^{-1}). Ammonia oxidation determined by the ^{15}N tracer method has not been reported in the subarctic open ocean or the BERS. In the Chukchi Sea, ammonia oxidation is recognized to be low in summer (0.2–0.4 nmolN l^{-1} h^{-1} (= 4.8–9.6 nmolN l^{-1} d^{-1})) (Baer *et al.*, 2014). We also observed low rates of ammonia oxidation in the BPLR (5.08 nmolN l^{-1} d^{-1}).

In ^{15}N tracer experiments for ammonia oxidation in the open ocean, ^{15}N-labeled ammonium is recognized to substantially increase the substrate concentration and may enhance ammonia oxidation (Clark *et al.*, 2008; Horak *et al.*, 2013; Newell *et al.*, 2013). Kinetics experiments performed in previous studies demonstrated that ammonia oxidation was stimulated with increasing concentration of ^{15}N-labeled ammonium (Horak *et al.*, 2013; Newell *et al.*, 2013). In our study, at Sts. 1–12, the substrate concentrations increased from 1.9 to 5.4 times by the addition of 31 nM ^{15}N-labeled ammonium. However, in the kinetic experiment, significant enhancement of ammonia oxidation was observed only at St. 12. These results suggest that ammonia oxidation reached a plateau below the minimum substrate concentration (31 nM added ^{15}N-labeled ammonium +ambient ammonium). Newell *et al.* (2013) reported a substantial increase in ammonia oxidation after the addition of 1.8–12 nM ^{15}N tracer. Hence, except at St. 12, AOO communities could have a high affinity for ammonia. In addition, the absence of a difference in ammonia oxidation after the addition of an excess amount of ^{15}N-labeled ammonium suggests that other factors could have influenced the AOO activity.

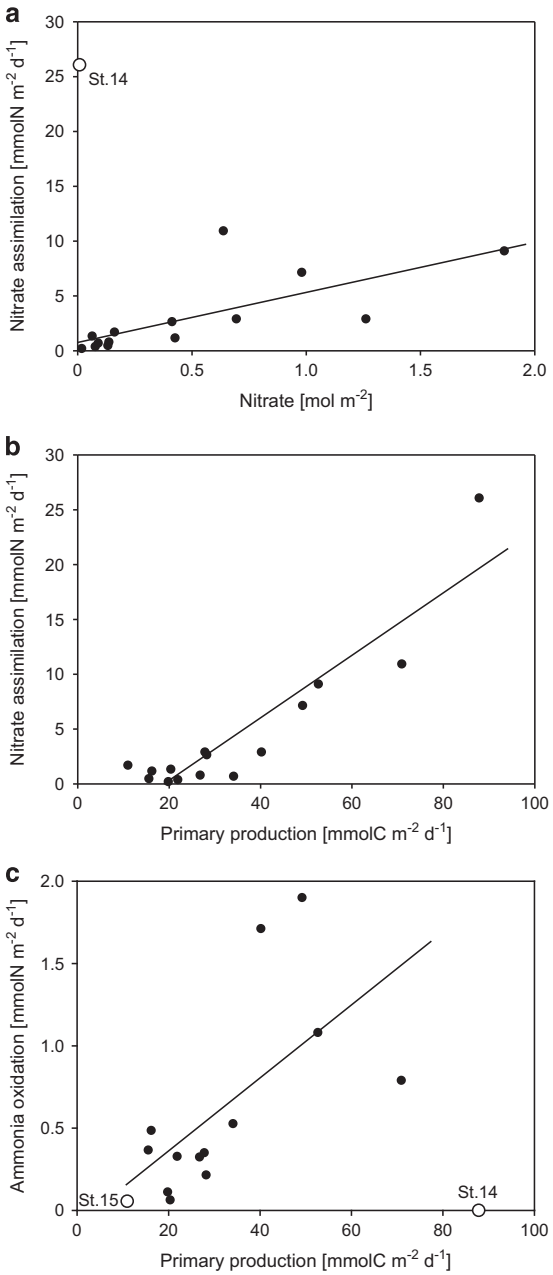

Figure 5 Relationships between (**a**) depth-integrated nitrate and nitrate assimilation, (**b**) depth-integrated primary production and nitrate assimilation and (**c**) depth-integrated primary production and ammonia oxidation. Open circles denote data excluded from the regression analysis (see text).

The maximum depth of ammonia oxidation generally occurred between the 1% and the 0.1% light depth and was placed below the SCM except at Sts. 13–15. Similar vertical profiles have been observed in previous studies of the South Pacific Ocean (Raimbault and Garcia, 2008; Raimbault *et al.*, 2008). AOA and AOB are both regulated in their activity by light (Olson, 1981; Guerrero and Jones, 1996; Merbt *et al.*, 2012). In contrast, phytoplankton has an extremely high ammonium affinity in surface water (Harrison *et al.*, 1996), and the ammonium assimilation activity decreases with light degradation (MacIsaac and Dugdale, 1972). Therefore, the difference between the depth of the SCM and the depth of the ammonia oxidation maximum is ascribable to the light environment and ammonium resource competition (c.f. Ward, 1985). In our study, the ammonia oxidation maximum occurred around the nitrite maximum, which corresponds with the results of previous reports (Raimbault and Garcia, 2008; Raimbault *et al.*, 2008; Beman *et al.*, 2008, 2012; Newell *et al.*, 2013; Santoro *et al.*, 2013). Although the formation of the nitrite maximum is considered to be due to ammonia oxidation (Santoro *et al.*, 2013) and/or the activity of phytoplankton (Lomas and Lipschultz, 2006), the data set obtained did not clarify which factor was essential.

The maximum abundance of shallow clade AOA was located above the depth of the maximum abundance of deep clade AOA throughout the study regions, the same trend reported in previous studies (Beman *et al.*, 2008; Smith *et al.*, 2014). At all stations, the *amoA* gene abundance of shallow clade AOA dominated in the AOO to the depth of 200 m, and the expression of shallow clade AOA at the 0.1% light depth exceeded those of deep clade AOA and βAOB, suggesting that shallow clade AOA was the major AOO in this study region. This inference was also supported by the fact that the *amoA* gene abundance and expression of shallow clade AOA were both positively correlated with ammonia oxidation. This relationship was also observed in a previous study (Smith *et al.*, 2014). It should be noted that variation in *amoA* expression of shallow clade AOA was not necessarily linked with gene abundance. For example, *amoA* gene abundance of shallow clade AOA at the 0.1% light depth at St.10 was comparable to that at St. 9, but the gene expression at St. 10 was about one-tenth that at St. 9. Furthermore, although the *amoA* gene of deep clade AOA (βAOB) was detected at the 0.1% light depth at Sts. 2–5, 8, 10 and 12 (Sts. 1, 7, 8, 10 and 15), it was not expressed there. Although these results were obtained at one sampling depth, the deviation between *amoA* gene abundance and gene expression could cause the difference in maximum depth between ammonia oxidation and AOO abundance.

The nitrate assimilation rates that we obtained were comparable to those of previous studies in each region (Supplementary Table S4). The concentrations of chlorophyll *a* and nitrate indicated that Sts. 10 and 11 were in the high-nutrient low-chlorophyll region, suggesting that biological production was limited by trace metals (particularly iron) (Boyd *et al.*, 2004; Moore *et al.*, 2013). The surface nitrate concentration at St. 10 was higher than that at St. 11. On the other hand, the chlorophyll *a* concentration and the nitrate assimilation at St. 10 were less than half those at St. 11. This suggests that biological production at St. 10 was likely more limited by iron than biological production at St. 11. St. 11 was located near the Aleutian Islands. Iron

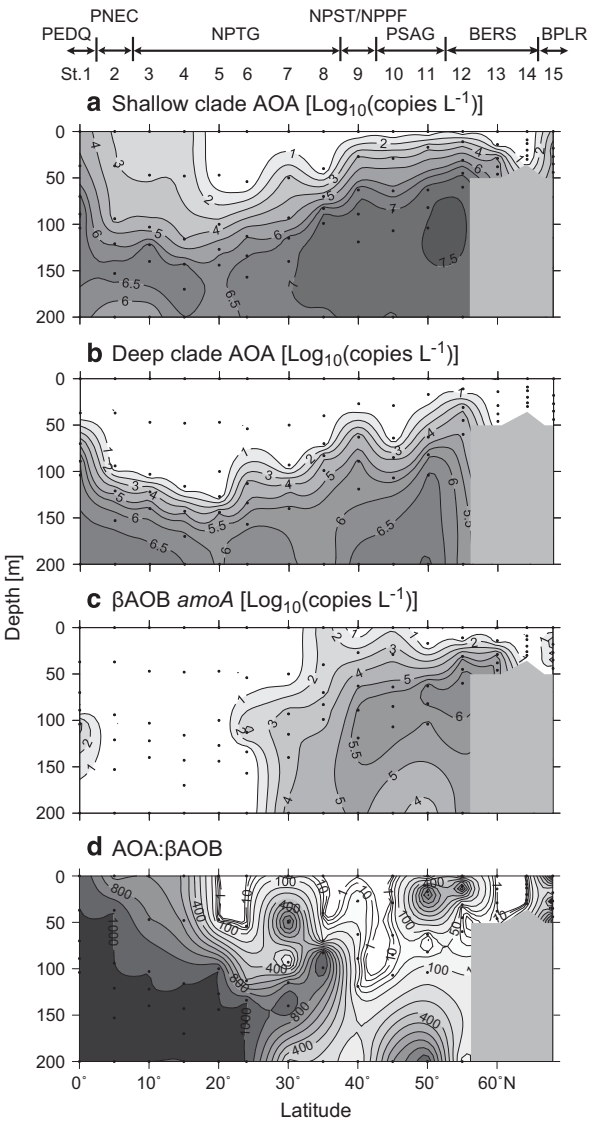

Figure 6 Vertical profiles of *amoA* abundance (Log_{10}(copies l^{-1})) of (**a**) shallow clade AOA, (**b**) deep clade AOA, (**c**) βAOB and (**d**) the ratio of shallow and deep clade AOA to βAOB (AOA:βAOB).

concentration near the Aleutian Islands (>0.4 nM) is considerably higher than in the subarctic gyre (<0.01 nM) (Suzuki *et al.*, 2002), and thus iron delivered from coastal water may have contributed to the production. Satellite-derived chlorophyll *a* indicated that active production occurred near the islands (Figure 1), which supports our inference. At St. 12, in the off-shelf area of the BERS, the surface nitrate assimilation (586 nmolN l^{-1} d^{-1}) was about six times higher than that at St. 9 (104 nmolN l^{-1} d^{-1}), whereas the surface nitrate concentration at St. 12 (435 nM) was similar to that at St. 9 (305 nM). St. 12 was located at the shelf edge and hence was probably in the Green Belt, which is defined as a highly productive region along the edge of the continental shelf of the Bering Sea (Springer *et al.*, 1996). Iron input to the Green Belt is high and enhances primary production (Aguilar-Islas *et al.*, 2007). Therefore, the elevated nitrate assimilation at St. 12 was ascribable to a higher iron supply than at St. 9. Nitrate assimilation was strongly related with primary production, suggesting that the biological production could be influenced by the supply of not only nitrate but also micronutrients.

When we assumed that ammonia and nitrite oxidations were tightly coupled, ammonia oxidation had a significant impact on nitrate assimilation, particularly in the subtropical region. A previous study in the South Pacific (Raimbault and Garcia, 2008) and a modeling study (Yool *et al.*, 2007) came to the same conclusion as we have presented. Raimbault and Garcia (2008) reported that the ratio of ammonia oxidation to nitrate assimilation was 80–100% in the subtropical South Pacific Ocean. Although this ratio in the subtropical region (PNEC and NPTG) was ca.80% at some stations, the average of 55.6% was lower than that in the subtropical South Pacific. The surface environment at Sts. 13–15 was also under oligotrophic conditions. However, the ammonia oxidation rates were low and the majority of nitrate assimilation was new production, suggesting that ammonia oxidation does not necessarily significantly influence the estimate of nitrate-based new production in all oligotrophic regions.

Environmental controls on the distribution of AOO and ammonia oxidation

Although βAOB was not detected0 or barely detected in the PNEC and NPTG, it was abundant from the NPST/NPPF to St. 13. The ammonium affinity of AOB is lower than that of AOA (Martens-Habbena *et al.*, 2009); thus, it would be difficult for AOB to survive in the oligotrophic unproductive region. The variation in βAOB abundance was likely due to the supply of ammonium. In fact, the relative abundance of βAOB in AOO has been reported to increase with ammonium concentration (Bouskill *et al.*, 2012; Urakawa *et al.*, 2014), and we had a similar result here. Distribution of microbial communities is influenced by physical structure and is described as stratified with depth (Giovannoni and Vergin, 2012). The mixed layer depth at Sts. 2–4 was deeper relative to that at the adjacent stations, and there was no significant regional difference at the other stations (Supplementary Figure S3a). Thus, the vertical distribution of AOO was not consistent with the mixed layer depth; rather, it was correlated with the euphotic depth, suggesting that light environment was an important factor in determining the vertical distribution of AOO. Some studies reported that oxygen concentration is also important for determining AOO distribution and their activities (Ward, 2002; Beman *et al.*, 2008; Bouskill *et al.*, 2012) and the AOO abundances and activities were reported to be high in the oxygen minimum zone (Beman *et al.*, 2008; Bouskill *et al.*, 2012). In the present study, although low-oxygen water was observed below 100 m at Sts. 2, 3 and 11 (Supplementary Figure S3b), AOO abundances and activities were

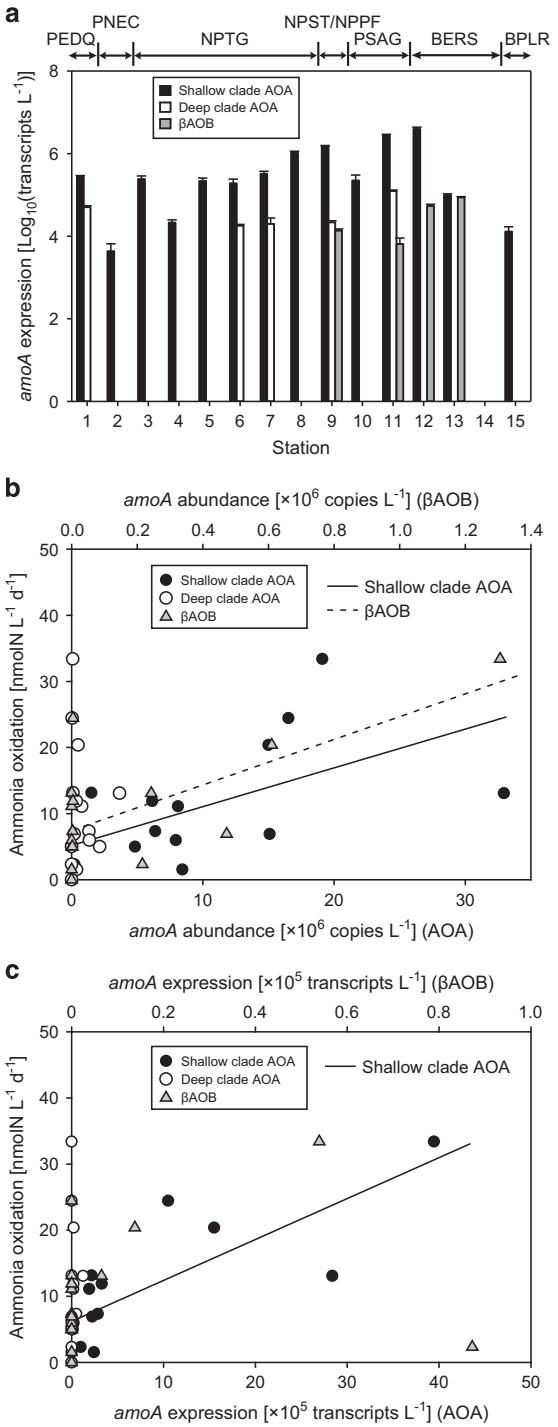

Figure 7 (**a**) Latitudinal variation in *amoA* expression (Log_{10} (transcripts l^{-1})) of shallow clade AOA, deep clade AOA, and βAOB at the 0.1% light depth (see dashed line in Figure 3b). Error bars indicate s.d.s of triplicate qPCR analyses. (**b, c**) Relationships at the 0.1% light depth between (**b**) *amoA* abundance of shallow clade AOA, deep clade AOA, and βAOB and ammonia oxidation and (**c**) *amoA* expression of shallow clade AOA, deep clade AOA and βAOB and ammonia oxidation.

not markedly high in these waters. Oxygen concentration above 100 m in the north of the PSAG increased, and it was not notably correlated with AOO abundance or activities. AOO abundance and ammonia oxidation were not detected at St. 14 and were low at St. 15. In the Arctic Ocean, nitrification activity was reported to be low in summer (Christman *et al.*, 2011; Baer *et al.*, 2014). Christman *et al.* (2011) and Baer *et al.* (2014) showed that chlorophyll *a* was high and ammonium concentration was low in summer and suggested that phytoplankton could outcompete AOO for ammonium resources. In our study, AOO abundance and activity were low in the region, but a high ammonium concentration was observed near the bottom. The existence of ammonium-rich water indicated that the low nitrification activity was not due simply to ammonium resource competition with phytoplankton. In the shelf region of BERS and BPLR, ammonium-rich water generally occurs near the bottom during summer as a result of active ammonia regeneration (Saino *et al.*, 1983; Whitledge *et al.*, 1986; Nishino *et al.*, 2005). As Christman *et al.* (2011) and Baer *et al.* (2014) collected their samples from 2–6.5 m, they missed sampling the ammonium-rich water. Such ammonium-rich (>1 μM) water masses are rarely observed in the ocean (Brzezinski, 1988; Rees *et al.*, 2006; Zhang *et al.*, 2007). This might also be influenced by the low ammonia oxidation and not only be due to the active ammonia regeneration.

The question of why AOO abundance and activity were low at Sts. 13–15 requires consideration. One of the possible factors is the light environment. Light is known to generally inhibit the activity of AOO (Olson, 1981; Guerrero and Jones, 1996; Merbt *et al.*, 2012). At. Sts. 14 and 15, the SCM occurred near the bottom, suggesting that the light environment was sufficient for the growth of phytoplankton. Therefore, it could make it difficult for AOO to survive, at least at Sts. 14 and 15. Furthermore, competition with other organisms for resources except ammonium and the existence of nitrification inhibitors could also influence the activities. This should be clarified in future studies.

When we excluded the data at Sts. 14 and 15, where nitrification was clearly suppressed by various factors, the depth-integrated ammonia oxidation rates were positively correlated with primary production ($r = 0.63$, $P < 0.05$) (Figure 5c). Substrate supply is generally considered to be essential for ammonia oxidation (Ward, 2002). This significant correlation suggests that ammonia oxidation was likely enhanced by high ammonium supply through decomposition of organic matter in highly productive water. However, our kinetics experiment demonstrated that ammonia oxidation did not increase significantly with additional ammonium of 31–1560 nM, except at St. 12. Although we performed the kinetics experiment at a single depth and results from other depths might differ, the obtained result implies that other factor(s), in addition to the difference in ammonium supply, could contribute to ammonia oxidation. As mentioned previously, the primary production and nitrate assimilation revealed

in this study would have been influenced by the supply of micronutrients. The shallow clade AOA was the major AOO in the study regions, and previous genome analyses have indicated that copper is probably important for ammonia oxidation by AOA (Walker *et al*., 2010; Hollibaugh *et al*., 2011). During our cruise, dissolved copper concentration at the SCM was low ($\leqslant$1.8 nM) at Sts. 1–10 and significantly increased in the BERS ($\geqslant$2.0 nM) (S. Takeda, pers. comm.). Previous studies also reported that dissolved copper concentration to the 200-m depth was $< \sim 2$ nM in the subarctic North Pacific (Fujishima *et al*., 2004; Takano *et al*., 2014), $< \sim 1$ nM in the subtropical North Pacific (Takano *et al*., 2014), and 2–10 nM in the Bering Sea (Cid *et al*., 2011). This distribution pattern is similar to that of iron (Fujishima *et al*., 2001; Cid *et al*., 2011), the supply of which likely limited primary production and nitrate assimilation. Considering this pattern, the lower ammonia oxidation at St. 10 in the subarctic ocean can be explained: it was attributable to a shortage of copper. In contrast, at St. 12, in the Green Belt, the copper supply would be high enough. Thus, the ammonia oxidation increased significantly with the addition of ammonium.

Conclusion

Although the contribution of nitrification to nitrate assimilation was significant in the subtropical oligotrophic region, it was low ($<$20%) in most of the other regions. The *amoA* gene abundance and expression of shallow clade AOA were the highest among the AOO from the equatorial Pacific to Arctic Ocean, indicating that shallow clade AOA was the major AOO in the study regions. The ratio of AOA to βAOB changed significantly with region, and it was related to ammonium concentration. Although AOO was detected even in the surface water, ammonia oxidation occurred mainly below the 1% light depth throughout the study region, indicating that it would be susceptible to light environment. Light was likely one of the reasons for very low ammonia oxidation in the shallow Bering and Chukchi Sea shelves. Ammonium concentration seemed to be important for determining the AOO community; however, it did not explain the distribution of ammonia oxidation. The kinetic experiments and the significant positive relationship between depth-integrated primary production and ammonia oxidation suggested that ammonia oxidation might be controlled by micronutrient (probably copper) availability. This was likely related with the fact that AOA, which require copper for ammonia oxidation (Walker *et al*., 2010; Hollibaugh *et al*., 2011), were dominant in the study regions.

Conflict of Interest

The authors declare no conflict of interest.

Acknowledgements

We thank H Ogawa, M Sato, D Sasano, R Shishikura, S Suzuki, and the captain, crew members and participants of the KH-14-3 cruise for their cooperation at sea. Thanks are also due to S Takeda for dissolved copper data during the KH-14-3 cruise. We acknowledge Y Sone, A Makabe and N Nakayama for their assistance in setting up the mass spectrometry instrument. We appreciate the NASA ocean color processing group for providing the chlorophyll *a* data set. This study was supported financially by MEXT Grants-in-Aid for Young Scientists (26850115), for JSPS Fellows (25-7341) and for Scientific Research on Innovative Areas (24121001, 24121003), by the Sasakawa Scientific Research Grant (26-746), and by the Japan Agency for Marine-Earth Science and Technology.

References

Aguilar-Islas AM, Hurst MP, Buck KN, Sohst B, Smith GJ, Lohan MC *et al.* (2007). Micro- and macronutrients in the southeastern Bering Sea: Insight into iron-replete and iron-deplete regimes. *Progr Oceanogr* **73**: 99–126.

Baer SE, Connelly TL, Sipler RE, Yager PL, Bronk DA. (2014). Effect of temperature on rates of ammonium uptake and nitrification in the western coastal Arctic during winter, spring, and summer. *Glob Biogeochem Cycles* **28**: 1455–1466.

Beman JM, Popp BN, Francis CA. (2008). Molecular and biogeochemical evidence for ammonia oxidation by marine Crenarchaeota in the Gulf of California. *ISME J* **2**: 429–441.

Behrenfeld MJ, Falkowski PG. (1997). Photosynthetic rates derived from satellite-based chlorophyll concentration. *Limnol Oceanogr* **42**: 1–20.

Beman JM, Popp BN, Alford SE. (2012). Quantification of ammonia oxidation rates and ammonia-oxidizing archaea and bacteria at high resolution in the Gulf of California and eastern tropical North Pacific Ocean. *Limnol Oceanogr* **57**: 711–726.

Bouskill NJ, Eveillard D, Chien D, Jayakumar A, Ward BB. (2012). Environmental factors determining ammonia-oxidizing organism distribution and diversity in marine environment. *Environ Microbiol* **14**: 714–729.

Boyd PW, Law CS, Wong CS, Nojiri Y, Tsuda A, Lavasseur M *et al.* (2004). The decline and fate of an iron-induced subarctic phytoplankton bloom. *Nature* **428**: 549–553.

Brzezinski MA. (1988). Vertical distribution of ammonium in stratified oligotrophic waters. *Limnol Oceanogr* **33**: 1176–1182.

Brochier-Armanet C, Boussau B, Gribaldo S, Forterre P. (2008). Mesophilic crenarchaeota: proposal for a third archaeal phylum, the Thaumarchaeota. *Nat Rev Microbiol* **6**: 245–252.

Church MJ, Wai B, Karl DM, DeLong EF. (2010). Abundances of crenarchaeal *amoA* genes and transcripts in the Pacific Ocean. *Environ Microbiol* **12**: 679–688.

Cid AP, Urushihara S, Minami T, Norisuye K, Sohrin Y. (2011). Stoichiometry among bioactive trace metals in seawater on the Bering Sea shelf. *J Oceanogr* **67**: 747–764.

Clark DR, Rees AP, Joint I. (2008). Ammonium regeneration and nitrification rates in the oligotrophic Atlantic Ocean: Implications for new production estimates. *Limnol Oceanogr* **53**: 52–62.

Christman GD, Cottrell MT, Popp BN, Gier E, Kirchman DL. (2011). Abundance, diverity, and activity of ammonia-oxidizing prokaryotes in the coastal Arctic Ocean in summer and winter. *Appl Environ Microbiol* **77**: 2026–2034.

Daims H, Lebedeva EV, Pjevac P, Han P, Herbold C, Albertsen M *et al.* (2015). Complete nitrification by *Nitrospira* bacteria. *Nature* **528**: 504–509.

Dugdale RC, Goering JJ. (1967). Uptake of new and regenerated forms of nitrogen in primary productivity. *Limnol Oceanogr* **12**: 196–206.

Eppley RW, Peterson BJ. (1979). Particulate organic matter flux and planktonic new production in the deep ocean. *Nature* **282**: 677–680.

Falkowski PG, Laws EA, Barber RT, Murray JW. (2003) Phytoplankton and their role in primary, new, and export production. In: Fasham MJR (ed). *Ocean Biogeochemistry*. Springer: New York, NY, USA, pp 99–121.

Francis CA, Roberts KJ, Beman JM, Santoro AE, Oakley BB. (2005). Ubiquity and diversity of ammonia-oxidizing archaea in water columns and sediments of the ocean. *Proc Natl Acad Sci USA* **102**: 14683–14688.

Fujishima Y, Ueda K, Maruo M, Nakayama E, Tokutome C, Hasegawa H *et al.* (2001). Distribution of trace bioelements in the subarctic North Pacific Ocean and the Bering Sea (the R/V Hakuho Maru Cruise KH-97-2). *J Oceanogr* **57**: 261–273.

Giovannoni SJ, Vergin KL. (2012). Seasonality in ocean microbial communities. *Science* **335**: 671–676.

Guerrero MA, Jones RD. (1996). Photoinhibition of marine nitrifying bacteria. I. Wavelength-dependent response. *Mar Ecol Prog Ser* **141**: 183–192.

Hallam SJ, Mincer TJ, Schleper C, Preston CM, Roberts K, Richardson PM *et al.* (2006). Pathways of carbon assimilation and ammonia oxidation suggested by environmental genomic analyses of marine *Crenarchaeota*. *PLoS Biol* **4**: 520–536.

Harrison WG, Harris LR, Irwin BD. (1996). The kinetics of nitrogen utilization in the oceanic mixed layer: Nitrate and ammonium interactions at nanomolar concentrations. *Limnol Oceanogr* **41**: 16–32.

Harrison PJ, Whitney FA, Tsuda A, Saito H, Tadokoro K. (2004). Nutrient and plankton dynamics in the NE and NW gyres of the subarctic Pacific Ocean. *J Oceanogr* **60**: 93–117.

Hashihama F, Furuya K, Kitajima S, Takeda S, Takemura T, Kanda J. (2009). Macro-scale exhaustion of surface phosphate by dinitrogen fixation in the western North Pacific. *Geophys Res Lett* **36**: L03610.

Hashihama F, Kanda J, Tauchi A, Kodama T, Saito H, Furuya K. (2015). Liquid waveguide spectrophotometric measurement of nanomolar ammonium in seawater based on the indophenol reaction with *o*-phenylphenol (OPP). *Talanta* **143**: 374–380.

Hollibaugh JT, Gifford S, Bano N, Sharma S, Moran MA. (2011). Matatranscriptomic analysis of ammonia-oxidizing organisms in an estuarine bacterioplankton assemblage. *ISME J* **5**: 866–878.

Horak REA, Qin W, Schauer AJ, Armbrust EV, Ingalls AE, Moffett JW *et al.* (2013). Ammonia oxidation kinetics and temperature sensitivity of a natural marine community dominated by Archaea. *ISME J* **7**: 2023–2033.

Hornek R, Pommerening-Röser A, Koops HP, Farnleiter AH, Kreuzinger N, Kirschner A *et al.* (2006). Primer containing universal bases reduce multiple *amoA* gene specific DGGE band patterns when analysing the diversity of beta-ammonia oxidizers in the environment. *J Microbiol Methods* **66**: 147–155.

Isobe K, Suwa Y, Ikutani J, Kuroiwa M, Makita T, Takebayashi Y *et al.* (2011). Analytical techniques for quantifying $^{15}N/^{14}N$ of nitrate, nitrite, total dissolved nitrogen and ammonium in environmental samples using a gas chromatograph equipped with a quadrupole mass spectrometer. *Microbes Environ* **26**: 46–53.

Kanda J, Itoh T, Ishizaka D, Watanabe Y. (2003). Environmental controls of nitrate uptake in the East China Sea. *Deep-Sea Res II* **50**: 403–422.

Kodama T, Ichikawa T, Hidaka K, Furuya K. (2015). A highly sensitive and large concentration range colorimetric continuous flow analysis for ammonium concentration. *J Oceanogr* **71**: 65–75.

Könneke M, Bernhard AE, de la Torre JR, Walker CB, Waterbury JB, Stahl DA. (2005). Isolation of an autotrophic ammonia-oxidizing marine archaeon. *Nature* **437**: 543–546.

Lomas MW, Lipschultz F. (2006). Forming the primary nitrite maximum: nitrifiers or phytoplankton? *Limnol Oceanogr* **51**: 2453–2467.

Longhurst AR. (2007). *Ecological Geography of the Sea*. 2nd edn. Academic Press: San Diego, CA, USA.

Merbt SN, Stahl DA, Casamayor EO, Marti E, Nicol GW, Prosser JI. (2012). Differential photoinhibition of bacterial and archaeal ammonia oxidation. *FEMS Microbiol Lett* **327**: 41–46.

Martens-Habbena W, Berube PM, Urakawa H, de la Torre JR, Stahl DA. (2009). Ammonia oxidation kinetics determine niche separation of nitrifying Archaea and Bacteria. *Nature* **461**: 976–979.

MacIsaac JJ, Dugdale RC. (1972). Interactions of light and inorganic nitrogen in controlling nitrogen uptake in the sea. *Deep-Sea Res* **19**: 209–232.

Moore CM, Mills MM, Arrigo KR, Berman-Frank I, Bopp L, Boyd PW *et al.* (2013). Processes and patterns of oceanic nutrient limitation. *Nat geosci 6*, 701–710.

Newell SE, Fawcett SE, Ward BB. (2013). Depth distribution of ammonia oxidation rates and ammonia-oxidizer commuity composition in the Sargasso Sea. *Limnol Oceanogr* **58**: 1491–1500.

Nishino S, Shimada K, Itoh M. (2005). Use of ammonium and other nitrogen tracers to investigate the spreading of shelf waters in the western Arctic halocline. *J Geophys Res* **110**: C10005.

Olson RJ. (1981). Differential photoinhibition of marine nitrifying bacteria: a possible mechanism for the formation of the primary nitrite maximum. *J Mar Res* **39**: 227–238.

Purkhold U, Pommerening-Röser A, Juretschiko S, Schmid MC, Koops HP, Wagner M. (2000). Phylogeny of all recognized species of ammonia oxidizer based on comparative 16SrRNA and *amoA* sequence analysis: Implications for molecular diversity surveys. *Appl Environ Microbiol* **66**: 5368–5382.

Raimbault P, Slawyk G, Boudjellal B, Coatanoan C, Conan P, Coste B *et al.* (1999). Carbon and nitrogen uptake and export in the equatorial Pacific at 150°W: evidence of an efficient regenerated production cycle. *J Geophys Res* **104**: 3341–3356.

Raimbault P, Garcia N. (2008). Evidence for efficient regenerated production and dinitrogen fixation in nitrogen-deficient waters of the South Pacific Ocean: impact on new and export production estimates. *Biogeosciences* **5**: 323–338.

Raimbault P, Garcia N, Cerutti F. (2008). Distribution of inorganic and organic nutrients in the South Pacific Ocean –evidence for long-term accumulation of organic matter in nitrogen-depleted waters. *Biogeosciences* **5**: 281–298.

Rees AP, Woodward EMS, Joint I. (2006). Concentrations and uptake of nitrate and ammonium in the Atlantic Ocean between 60°N and 50°S. *Deep-Sea Res II* **53**: 1649–1665.

Ryther JH. (1956). Photosynthesis in the ocean as a function of light intensity. *Limnol Oceanogr* **1**: 61–70.

Saino T, Otobe H, Wada E, Hattori A. (1983). Subsurface ammonium maximum in the northern North Pacific and the Bering Sea in summer. *Deep-Sea Res* **30**: 1157–1171.

Santoro AE, Sakamoto CM, Smith JM, Plant JN, Gehman AL, Worden AZ *et al.* (2013). Measurements of nitrite production in and around the primary nitrite maximum in the central California Current. *Biogeosciences* **10**: 7395–7410.

Shiozaki T, Furuya K, Kodama T, Takeda S. (2009). Contribution of N_2 fixation to new production in the western North Pacific Ocean along 155°E. *Mar Ecol Progr Ser* **377**: 19–32.

Shiozaki T, Furuya K, Kurotori H, Kodama T, Takeda S, Endoh T *et al.* (2011). Imbalance between vertical nitrate flux and nitrate assimilation on a continental shelf: Implications of nitrificaiton. *J Geophys Res* **116**: C10031.

Sigman DM, Casciotti KL, Andreani M, Barford C, Galanter M, Bohlke JK. (2001). A bacterial method for the nitrogen isotopic analysis of nitrate in seawater and freshwater. *Anal Chem* **73**: 4145–4153.

Smith JM, Casciotti KL, Chavez FP, Francis CA. (2014). Differential contributions of archaeal ammonia oxidizer ecotypes to nitrificaiton in coastal surface waters. *ISME J* **8**: 1704–1714.

Springer AM, McRoy CP, Flint MV. (1996). The Bering Sea Green Belt: shelf-edge processes and ecosystem production. *Fish Oceanogr* **5**: 205–223.

Suzuki K, Liu H, Saino T, Obata H, Takano M, Okamura K *et al.* (2002). East-west gradients in the photosynthetic potential of phytoplankton and iron concentration in the subarctic Pacific Ocean during early summer. *Limnol Oceangr* **47**: 1581–1594.

Takano S, Tanimizu M, Hirata T, Sohrin Y. (2014). Isotopic constraints on biogeochemical cycling of copper in the ocean. *Nat Comm* **5**: 5663.

Urakawa H, Martens-Habbena W, Huguet C, de la Torre JR, Ingalls AE, Devol AH *et al.* (2014). Ammonia availability shapes the seasonal distribution and activity of archaeal and bacterial ammonia oxidizers in the Puget Sound Estuary. *Limnol Oceanogr* **59**: 1321–1335.

van Kessel MAH, Speth DR, Albertsen M, Nielsen PH, Op den Camp HJM, Kartal B *et al.* (2015). Complete nitrification by a single microorganism. *Nature* **528**: 555–559.

Walker CB, de la Torre JR, Klots MG, Urakawa H, Pinel N, Arp DJ *et al.* (2010). Nitrosopumilus maritimus genome reveals unique mechanisms for nitrification and autotrophy in globally distributed marine crenarchaea. *Proc Natl Acad Sci USA* **107**: 8818–8823.

Ward BB. (1985). Light and substrate concentration relationships with marine ammonium assimilation and oxidation rates. *Mar Chem* **16**: 301–316.

Ward BB, Kilpatrick KA, Renger EH, Eppley RW. (1989). Biological nitrogen cycling in the nitracline. *Limnol Oceanogr* **34**: 493–513.

Ward BB. (2002). Nitrification in aquatic systems. In: Capone DA (ed). *Encyclopedia of Environmental Microbiology*. Wiley: New York, NY, USA, pp 2144–2167.

Whitledge TE, Reeburgh WS, Walsh JJ. (1986). Seasonal inorganic nitrogen distributions and dynamics in the southeastern Bering Sea. *Cont Shelf Res* **5**: 109–132.

Wuchter C, Abbas B, Coolen MJL, Herfort L, van Bleijswijk J, Timmers P *et al.* (2006). Archaeal nitrification in the ocean. *Proc Natl Acad Sci USA* **103**: 12317–12322.

Yool A, Martin AP, Fernández C, Clark DR. (2007). The significance of nitrification for oceanic new production. *Nature* **447**: 999–1002.

Zhang J, Liu SM, Ren JL, Wu Y, Zhang GL. (2007). Nutrient gradients from the euphotic Changjiang (Yangtze River) estuary to the oligotrophic Kuroshio waters and re-evaluation of budgets for the East China Sea Shelf. *Progr Oceanogr* **74**: 449–478.

Supplementary Information accompanies this paper on The ISME Journal website (http://www.nature.com/ismej)